

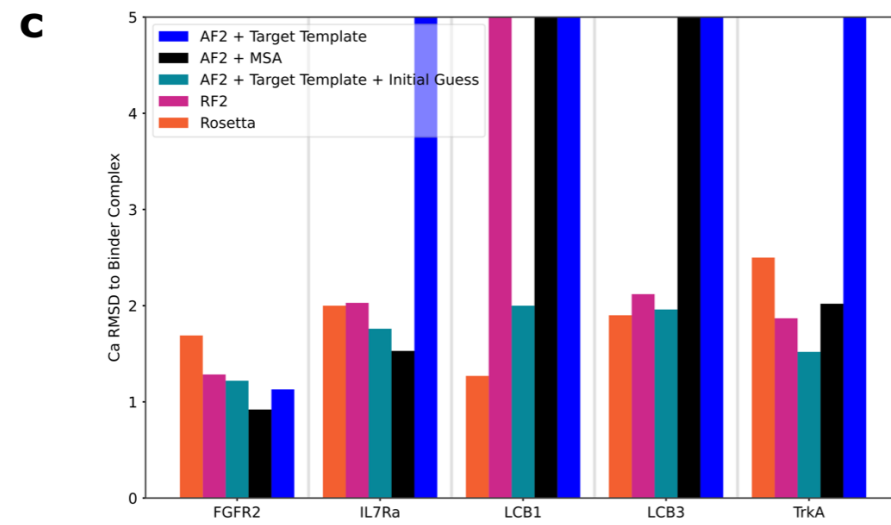
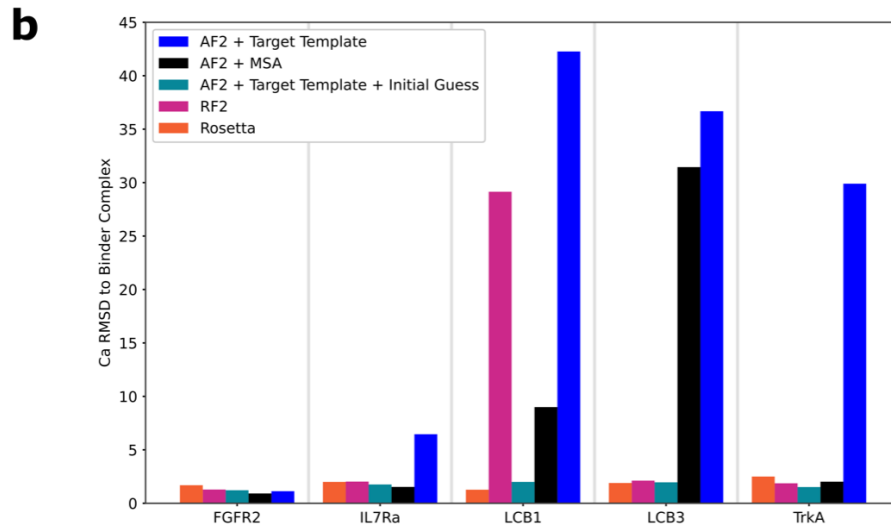
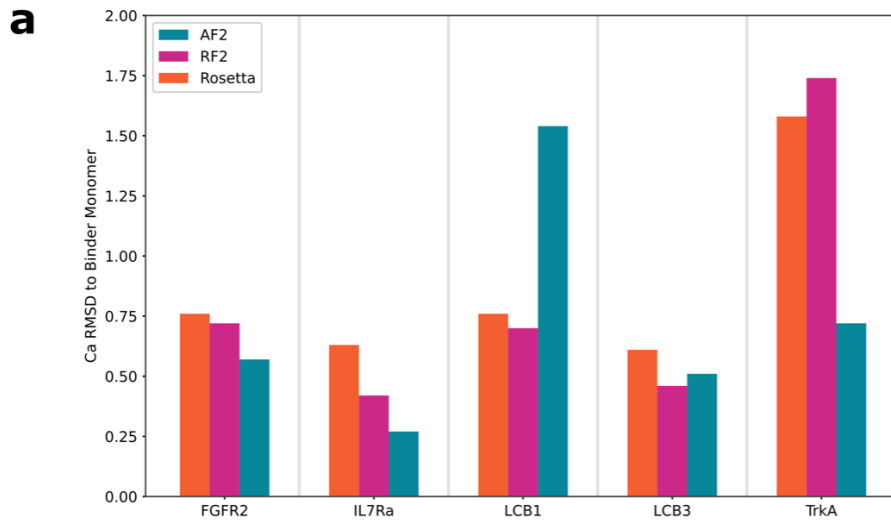
Supplementary Information for

Improving *de novo* Protein Binder Design with Deep Learning

Nathaniel R. Bennett^{1,2,3‡}, Brian Coventry^{1,2,4‡}, Inna Goreschnik^{1,2}, Buwei Huang^{1,2,5}, Aza Allen^{1,2}, Dionne Vafeados^{1,2}, Ying Po Peng^{1,2}, Justas Dauparas^{1,2}, Minkyung Baek^{1,2}, Lance Stewart^{1,2}, Frank DiMaio^{1,2}, Steven De Munck^{6,7}, Savvas N. Savvides^{6,7}, David Baker^{1,2,4*}

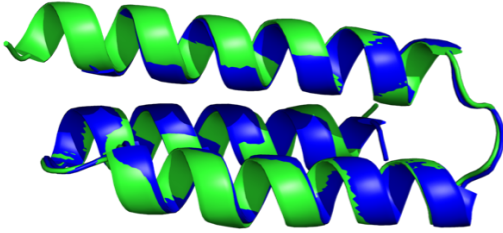
* Corresponding author. Email: dabaker@uw.edu

Supplementary Figures

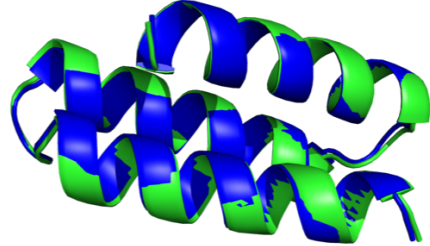


Supplementary Figure 1. **AF2 Prediction of Experimentally Determined Minibinder Structures.** **a** The accuracy in C α RMSD of AF2 and RF2 predictions of binder monomer structure for the five minibinder complex structures reported in Cao et al. **b** The accuracy in C α RMSD of AF2 and RF2 predictions of binder complex structure for the five minibinder complex structures reported in Cao et al. **c** A close-up view of B. Source data are provided as a Source Data file.

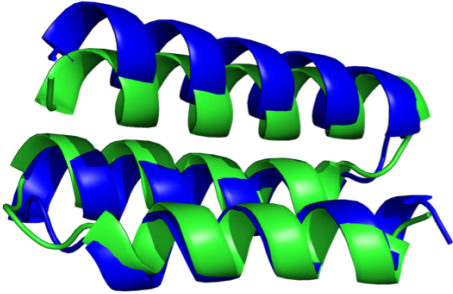
a



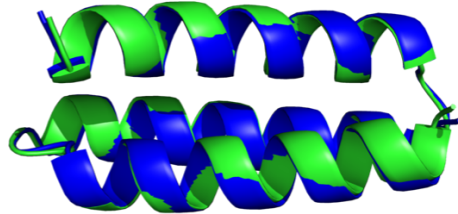
b



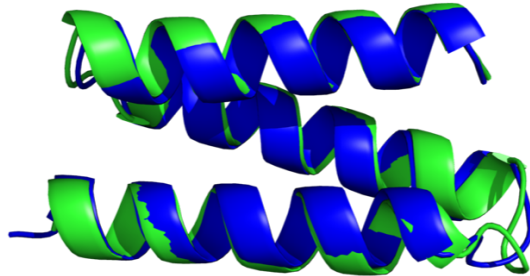
c



d



e

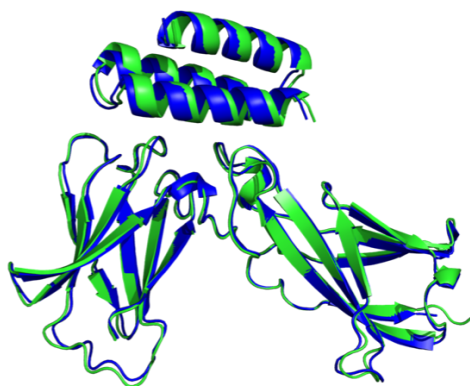


Supplementary Figure 2. **AF2 Monomer Predictions (Blue) are close to the Experimentally Determined Structures (Yellow).** **a** FGFR2 **b** IL-7R α **c** SARS-CoV-2 Spike (LCB1) **d** SARS-CoV-2 Spike (LCB3) **e** TrkA. Source data are provided as a Source Data file.

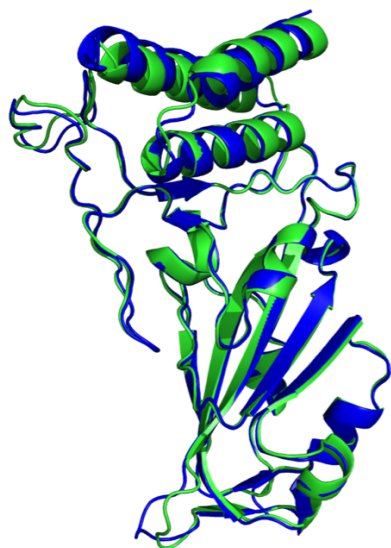
a



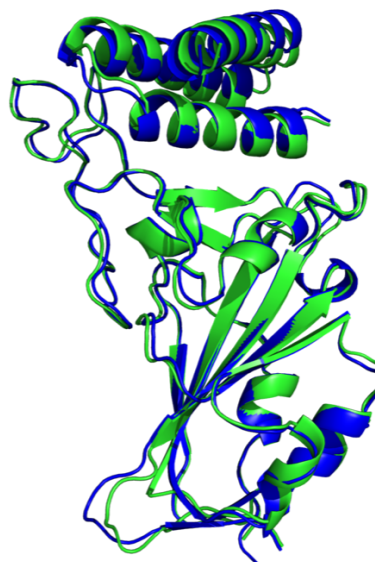
b



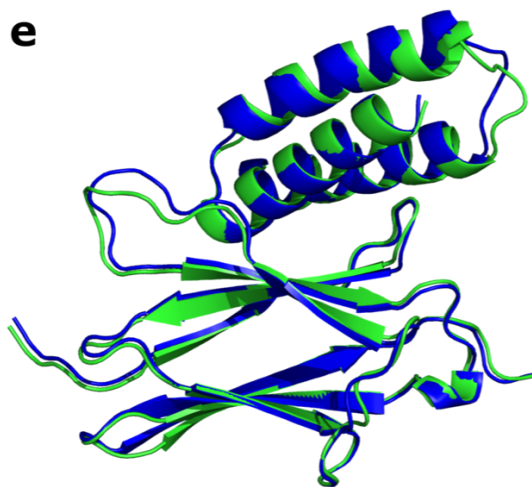
c



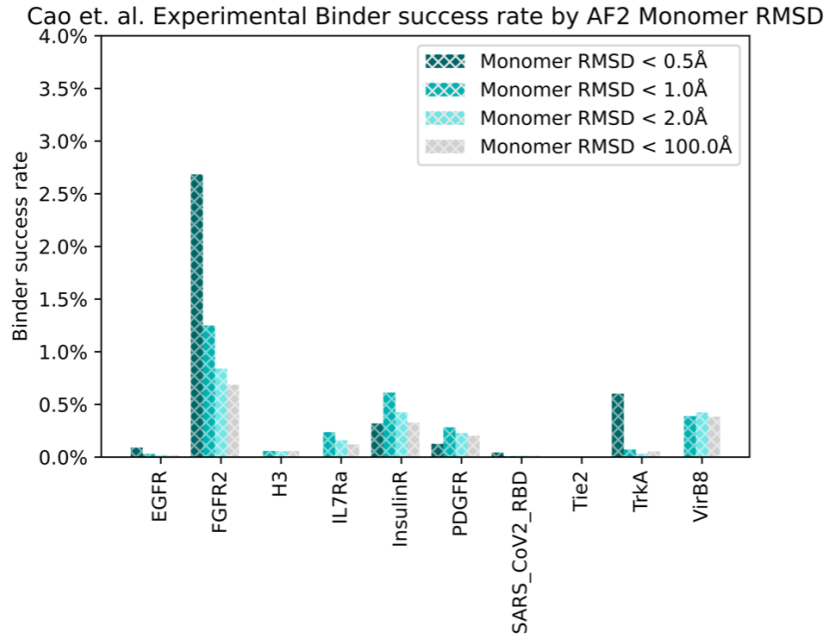
d



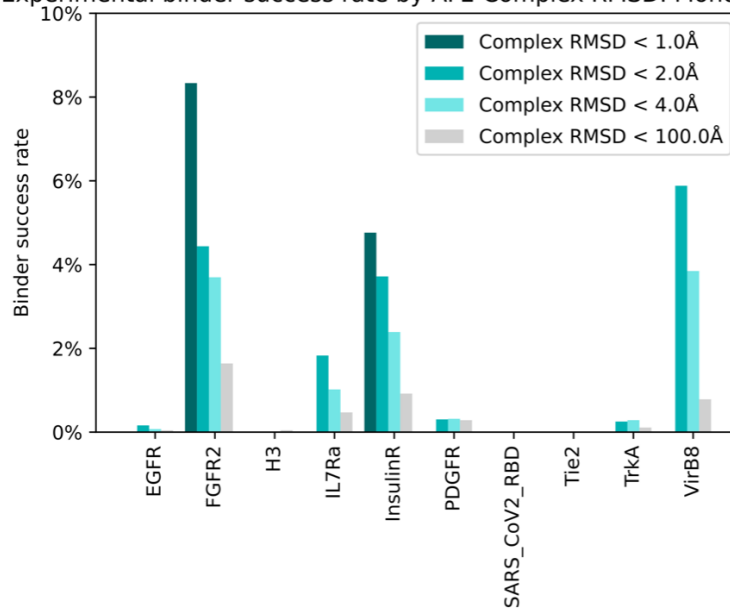
e



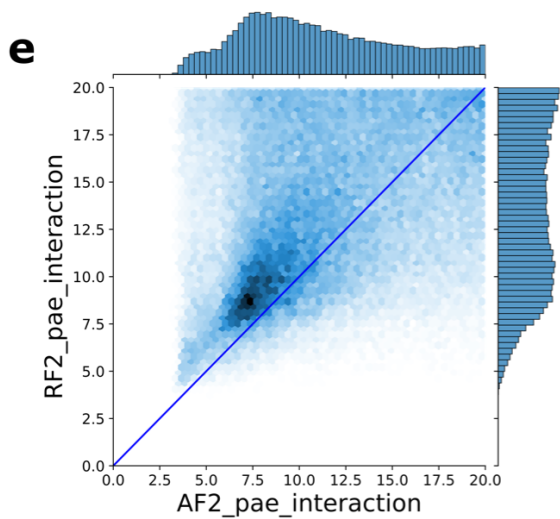
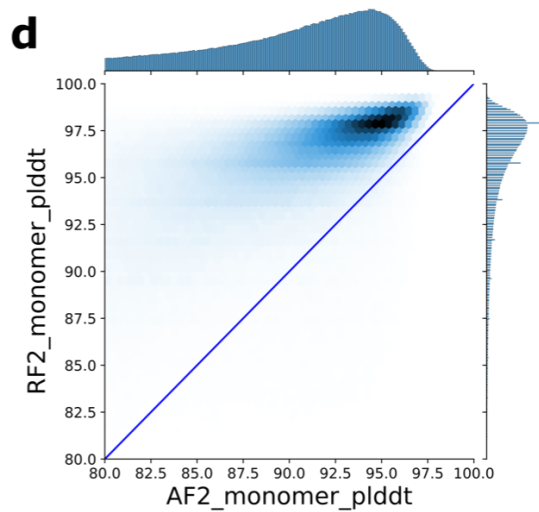
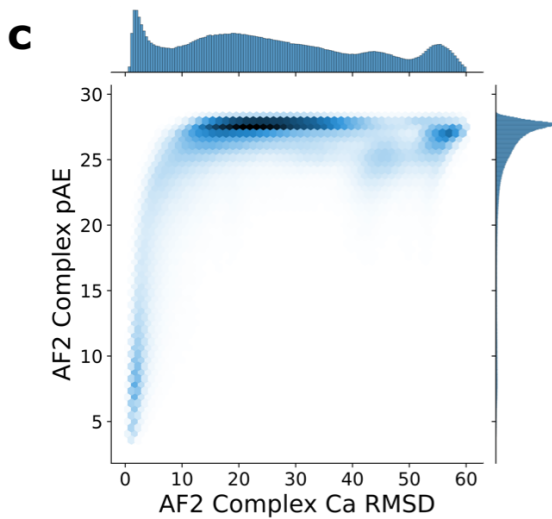
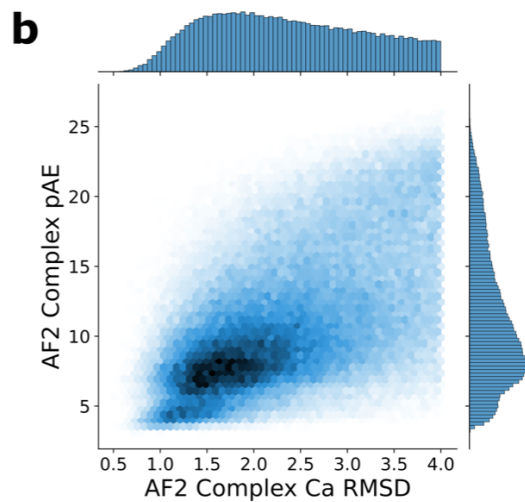
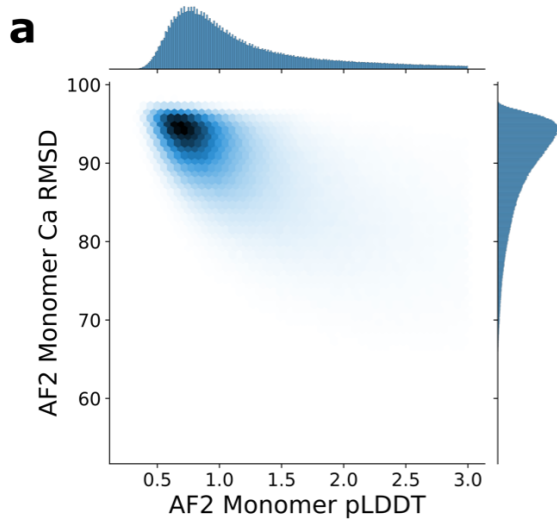
Supplementary Figure 3. **AF2 Complex Predictions (Blue) are close to the Experimentally Determined Structures (Yellow)**. All complex predictions shown were run using AF2 with target template and the Rosetta-design model as an initial guess. **a** FGFR2 **b** IL-7R α **c** SARS-CoV-2 Spike (LCB1) **d** SARS-CoV-2 Spike (LCB3) **e** TrkA. Source data are provided as a Source Data file.

a**b**

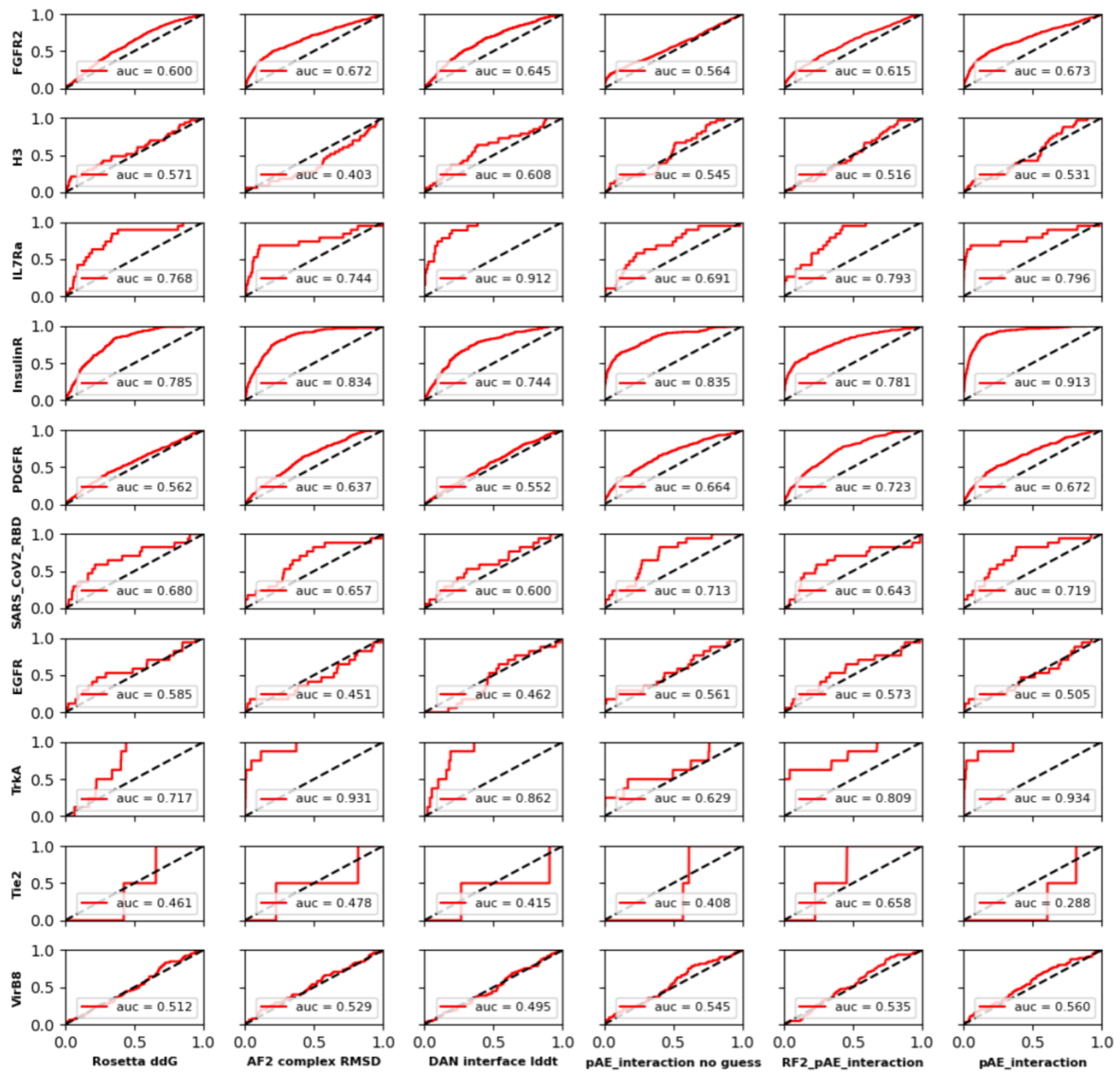
Cao et. al. Experimental binder success rate by AF2 Complex RMSD. Monomer RMSD < 0.75Å



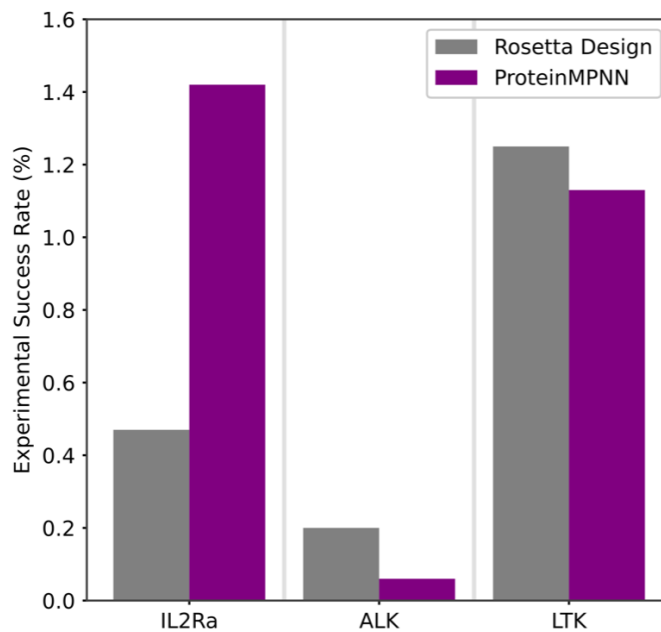
Supplementary Figure 4. **Retrospective Analysis of RMSD Metrics.** **a** The retrospective experimental success rate (YSD $SC_{50} < 4\mu\text{M}$) for designs passing 4 thresholds of the RMSD difference between the Rosetta monomer structure and the AF2 monomer structure. **b** The retrospective experimental success rate (YSD $SC_{50} < 4\mu\text{M}$) for designs passing 4 thresholds of the RMSD difference between the Rosetta complex structure and the AF2 complex structure. Source data are provided as a Source Data file.



Supplementary Figure 5. **Correlation Between AF2 Confidence Metrics and AF2 RMSD.** **a** For all binders in the dataset from Cao et al. the AF2 monomer confidence (pLDDT) and the RMSD difference between the Rosetta binder structure and the AF2 binder structure is plotted. **b** For all binders in the dataset from Cao et al. the AF2 complex confidence (pAE_interaction) and the RMSD difference between the Rosetta complex structure and the AF2 complex structure is plotted. **c** Zoomed-out version of (**b**). **d** For all binders in the dataset from Cao et al. the AF2 monomer confidence (AF2_monomer_plddt) and the RF2 monomer confidence (RF2_monomer_plddt) is plotted. The line $x=y$ is plotted in solid blue. **e** For all binders in the dataset from Cao et al. the AF2 complex confidence (AF2_pAE_interaction) and the RF2 complex confidence (RF2_pAE_interaction) is plotted. The line $x=y$ is plotted in solid blue. Source data are provided as a Source Data file.

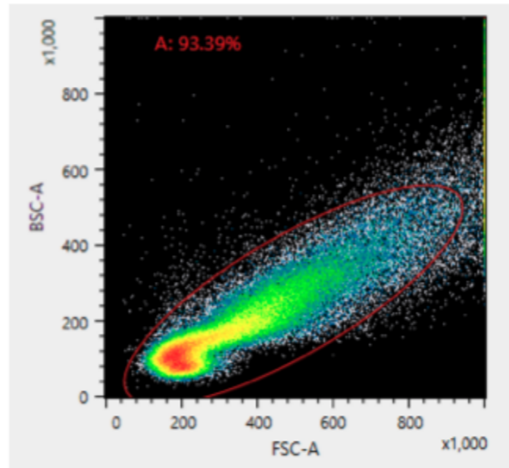


Supplementary Figure 6. **Retrospective Analysis of Complex Metrics.** For each combination of 10 targets and 6 interface metrics a Receiver-Operator Characteristic curve quantifying the discriminatory power of the metric to separate successful designs ($SC_{50} < 4 \mu\text{M}$) from unsuccessful designs ($SC_{50} \geq 4 \mu\text{M}$) is plotted. The True Positive Rate is plotted on the y-axis and the False Positive Rate on the x-axis. The Area Under the Curve (AUC) is included for each plot. Source data are provided as a Source Data file.

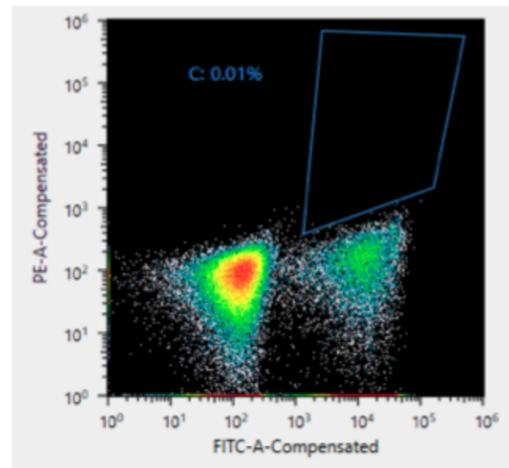


Supplementary Figure 7. **Experimental Success Rate of Binders Generated by ProteinMPNN versus Rosetta Design.** The experimental success rate for libraries generated by redesign of DL filtered designs with Rosetta FastDesign versus ProteinMPNN and filtered by DL-based filtering for three prospective targets. Source data are provided as a Source Data file.

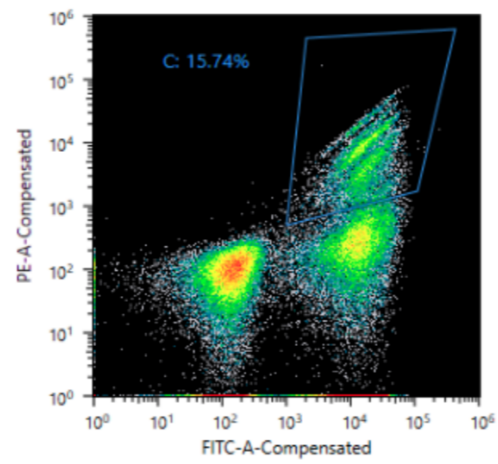
a



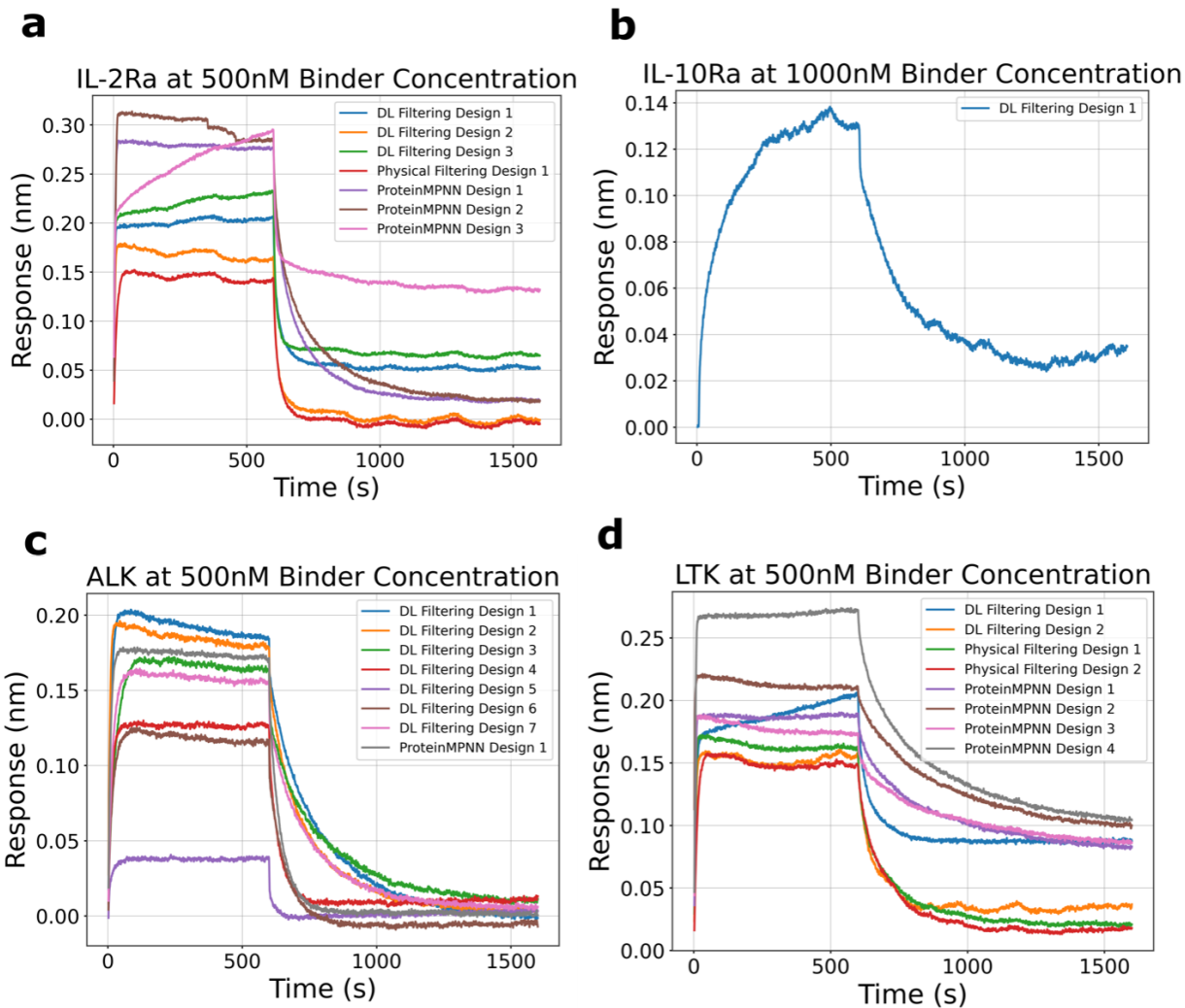
b



c



Supplementary Figure 8. **Gating Strategy for FACS Sorting of ALK Binder Library.** **a** Forward scatter (FSC) versus back scatter (BSC) plot with gate used in red. **b** Negative sort with gate shown in blue. **c** Binding sort with gate (same gate as used in **(b)**) shown in blue. Source data are provided as a Source Data file.



Supplementary Figure 9. **Biophysical Characterization of Select Designs.** For each target, 7-8 designs to that target, which showed binding by Yeast Surface Display, were screened for binding by single-concentration Biolayer Interferometry (BLI). For IL-10Ra only one design was identified and that is the only design which was screened by BLI. All designs tested showed binding signal by BLI. No successful ProteinMPNN designs against IL-10Ra were identified and only one successful ProteinMPNN design was identified to bind ALK. Source data are provided as a Source Data file.